Journal of Materials Chemistry B

PAPER

View Article Online
View Journal | View Issue

Cite this: J. Mater. Chem. B, 2014, 2, 511

Development of an efficient immobilization matrix based on a conducting polymer and functionalized multiwall carbon nanotubes: synthesis and its application to ethanol biosensors

Saniye Soylemez,[a] Fulya Ekiz Kanik,[b] Sema Demirci Uzun,[c] Serife O. Hacioglu[a] and Levent Toppare*[abcd]

Received 30th September 2013
Accepted 18th November 2013

DOI: 10.1039/c3tb21356k

www.rsc.org/MaterialsB

Material modification is one of the hot topics recently. Hereby a novel functional monomer, 2-(4-nitrophenyl)-4,7-di(thiophen-2-yl)-1*H*-benzo[*d*]imidazole (BIPN), was synthesized for matrix generation through electrochemical polymerization. Its conducting polymer was successfully used for the biolayer construction in the biosensor preparation. The electrochemical and morphological properties were improved by the introduction of carboxylic acid functionalized multiwall carbon nanotubes (f-MWCNTs). Carboxylic acid functionalization of MWCNTs was carried out *via* acid treatment. The electrode surface was modified with the polymer and f-MWCNTs during electropolymerization to achieve a perfect immobilization matrix for alcohol oxidase. In order to prepare a new alcohol biosensor, alcohol oxidase (AOx) was immobilized onto the modified electrode. The modified electrode was characterized by scanning electron microscopy (SEM), X-ray photoelectron microscopy (XPS) and Fourier transform infrared (FTIR) spectroscopy techniques. Electrochemical responses of the enzyme electrodes were monitored at −0.7 V *vs.* Ag reference electrode by monitoring oxygen consumption in the presence of ethanol. Kinetic parameters, operational and storage stabilities were investigated. K_M^{app}, I_{max}, LOD and sensitivity were calculated as 16.946 mM, 3.31 μA, 0.806 mM and 476 μA mM^{-1} cm^{-2}, respectively. Finally, this biosensor was applied to estimate the alcohol content in various beverages successfully.

1. Introduction

Material design is important in surface modification depending on the purpose of the application. Rather than using a pristine material, creating a modified one for a target application and tuning the material properties to make it useful for a certain purpose is a worthy step in scientific progress. Conducting polymers are materials which fulfil these properties due to their tunable and easy production for specific purposes. Conducting polymers (CPs) are recommended for their superior properties to serve as materials in different kinds of technological applications in electrochromic devices,[1] lithium ion batteries[2] and enzyme immobilization.[3] CPs provide high surface area, adjustable morphology depending on the thickness of the film, as well as well-organized suitable platform for enzyme immobilization. Moreover, CPs have functional groups, which provide maximum enzyme loading through the interaction between the enzyme molecule and functional groups of the polymers. With the help of these interactions, well organized platforms for biosensors can be achieved. Hence, functionalized conducting polymers are favorable materials and can be used for biomolecules.[4]

Carbon nanotubes (CNTs) are important nanomaterials for their incorporation into electrochemical and biological sensing devices due to fast electron transfer, high surface area, electrochemical stability and biocompatibility.[5] Moreover, CNTs can act as immobilization matrices and as electrochemical transducers, resulting in the improvement of performance of the immobilized enzyme which enhances their use in biosensors.[6a,b] CNTs are classified as single wall carbon nanotubes (SWCNTs) and multiwall carbon nanotubes (MWCNTs) which have the advantages of good dispersion and low cost. So far, most studies have focused on the development of an effective immobilization matrix using f-MWCNTs.[7] The functionalization of CNTs is an effective way to prevent nanotube aggregation, which helps to better disperse and stabilize the CNTs within solvent and a polymer matrix. The dispersion properties of CNTs can be improved by sidewall modification of nanotubes. Functionalization is the one of the most effective

[a]Department of Chemistry, Middle East Technical University, Ankara 06800, Turkey
[b]Department of Biotechnology, Middle East Technical University, Ankara 06800, Turkey
[c]Department of Polymer Science and Technology, Middle East Technical University, Ankara 06800, Turkey
[d]The Center for Solar Energy Research and Application (GUNAM), Middle East Technical University, Ankara 06800, Turkey

methods where strong oxidants (HNO_3 and H_2SO_4) are used to oxidize defect sites on the CNTs to produce hydrophilic groups.[8] Furthermore, the most promising step in biosensor preparation is enzyme immobilization. For preparation of mechanically robust and stable biosensors CNTs with the superior electron transfer properties are considered as appropriate electron transfer agents between the redox side of the enzyme molecules and the electrode.

The detection of ethanol with high sensitivity, selectivity and accuracy plays an important role in the quality control of alcoholic beverages as well as clinical analysis. Many analytical methods have been proposed for ethanol determination, which are poorly selective, expensive and time consuming. On the other hand, enzyme amperometric biosensors are very attractive due to the characteristics of the biocomponent specificity and the high sensitivity.[9] AOx from Pichiapastoris (EC 1.1.3.13) is one of the most used enzymes due to its substrate specificity and availability and stability over a useful range of reaction conditions, which makes this enzyme a promising catalyst for biosensor applications.[10a,b] AOx is the oligomeric flavoprotein with eight identical sub-units containing flavin adenine dinucleotide molecule (FAD) as the cofactor. AOx from Pichiapastoris catalyzes the oxidation of low molecular weight alcohols to aldehydes in the presence of molecular oxygen. During this reaction, the AOx cofactor (FAD) is first reduced to its hydrogenated form ($FADH_2$) and re-oxidized to its native form by molecular oxygen resulting in the formation of hydrogen peroxide.[11] The proposed biosensor working principle is based on Scheme 1.

In this study, with these motivations, a novel DAD type monomer, 2-(4-nitrophenyl)-4,7-di(thiophen-2-yl)-1*H*-benzo[*d*]-imidazole (BIPN), was synthesized and its polymer was successfully synthesized electrochemically. The novel benzimidazole containing polymer was thought to be used in biosensor application. Alcohol oxidase was immobilized onto the conducting polymer coated electrode to construct the biosensor. To improve the immobilization and enhance the interaction between the polymer and enzyme molecules, carboxylic acid functionalized multiwall carbon nanotubes (f-MWCNTs) were introduced within the polymer coat. By this way, not only covalent immobilization between the enzyme and carboxylic acid functionalized carbon nanotubes was provided to enhance the immobilization and prolong the stability, but also fast electron transfer on the electrode surface was achieved. Hence, the electrochemical properties of the polymer and the performance of the biosensor were improved. We developed a sensitive, simple and effective matrix for the preparation of an alcohol biosensor. The use of a conducting polymer of BIPN as the host matrix for immobilization of AOx enhanced the sensitivity, stability and film quality. Besides, the electrogenerated polymer film provides an easy control over the properties of the polymeric coat such as morphology and thickness.[12] Also, CNTs have attracted enormous interest due to their excellent electron transfer properties for oxidase-based amperometric biosensors.[13] CNTs and CPs are both interesting for their unique electrochemical properties. Without CNTs, the thin conducting polymer films provide a reasonable amperometric response time, but they can suffer from low conductivities. On the other hand, when the thickness of the polymeric film increases, charge transport between the active side of the enzyme molecule and the transducer becomes slow. To overcome these problems efficient binding between enzyme molecules and immobilization matrix was achieved with the combination of CPs and functionalized CNTs. The presence of –COOH or –OH groups on the nanotube surface improves the attachment of organic or inorganic materials since a variety of chemical reactions can be conducted with this group. Moreover, wrapping of functional CNTs in polymeric chains was found to be useful to improve their solubility as well as prevent nanotube aggregation, which helps to disperse and stabilize the CNTs in a polymer matrix.[14] With the help of the combination of CNTs, ordered and homogeneous free defect films have been easily achieved.[12] This combination process is constructed through the van der Waals interactions and π–π stacking between CNTs and polymer chains. Conducting polymers are attached to CNT surfaces by *in situ* polymerization to improve the processability, and electrical, magnetic and optical properties of CNTs. AOx was immobilized onto the CNT modified conducting polymer coated graphite electrode with the help of EDC/NHS crosslinking agents in order to construct an amperometric alcohol biosensor. The presence of the free carboxylic acid groups on the nanotube backbone can be utilized for the covalent attachment of enzymes *via* formation of amide bonds. In this case, 1-ethyl-3-(3-dimethylaminopropyl)carbodiimide (EDC) and *N*-hydroxysuccinimide (NHS) were used to activate the free carboxylic acid groups of the conducting nanotube backbone.[15] Through functional carboxylic acid groups of the CNT, amide bond formation between enzyme molecules and CNTs was generated. In addition to this

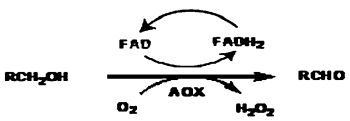

Scheme 1 Working principle of AOx.

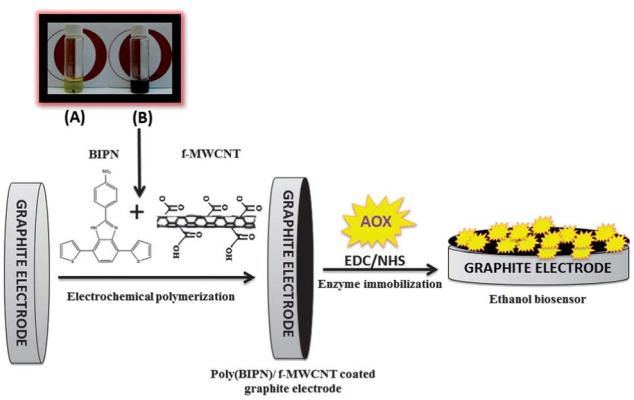

Scheme 2 Typical preparation of the proposed biosensor ((A) before and (B) after dispersibility behavior of f-MWCNTs in BIPN monomer solution given as the inset).

covalent binding, the physical adsorption process occurs where the enzyme molecules were adsorbed in the polymer interface due to π–π stacking and the hydrogen bond between the functional groups of the enzyme molecule and NO_2 of the conducting polymer. Therefore, the research is increasingly focused on the preparation of a novel immobilization matrix with the combination of CNTs and conducting polymer. Moreover, the affinity of biological molecules to the benzimidazole unit is well-known. This idea was also used while synthesizing the monomer. By this way, it was aimed to have a polymeric immobilization matrix with high affinity to enzyme molecules in order to well immobilize them onto the electrode surface. This allows better contact between the biomolecule and the electroactive layer thereby improving the biocompatibility of enzyme molecules. A representative preparation of the proposed biosensor is depicted in Scheme 2. The immobilization matrix was characterized by scanning electron microscopy (SEM), Fourier transform infrared (FTIR) spectroscopy and X-ray photoelectron microscopy (XPS) techniques. The practical application of this modified electrode was tested *via* determining alcohol in various beverages.

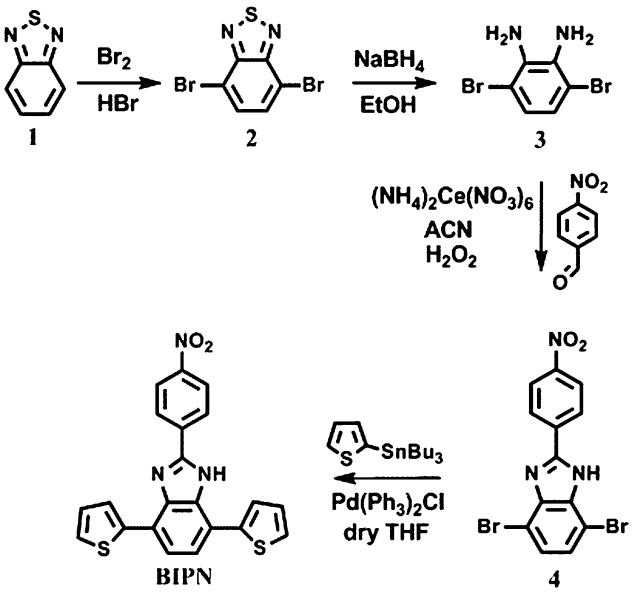

Scheme 3 Synthetic pathway of the corresponding monomer (BIPN).

2. Experimental

2.1 Materials

Alcohol oxidase (E.C.1.1.3.13) from Pichiapastoris (28 units per mg protein), methanol, $NaClO_4$ and $LiClO_4$ were purchased from Sigma-Aldrich and used with no further purification. Dichloromethane (DCM), acetonitrile (ACN) were purchased from Merck (Darmstadt, Germany). 2-Propanol and *tert*-butanol were obtained from (Merck). Ethanol (Carlo Erba) was used as received to prepare the substrate solution (1.7 M) at room temperature. For enzyme immobilization, a phosphate buffer solution (pH 7.0) consisting of 0.025 M Na_2HPO_4 (Fisher Scientific Company) and 0.025 M NaH_2PO_4 (Fisher Scientific Company) was used. *N*-Hydroxysuccinimide (NHS) and *N*-(3-dimethylaminopropyl)-*N*′-ethylcarbodiimide hydrochloride (EDC) were purchased from Fluka (Buchs, Switzerland) and Sigma, respectively. All chemicals were of analytical reagent grade. Bromine, 2,1,3-benzothiadiazole, ammonium cerium(IV) nitrate, ethyl acetate, chloroform, dichloromethane, bis-(triphenylphosphine)palladium(II) dichloride, 4-nitrobenzaldehyde, thiophene, *n*-butyllithium solution (2.5 M in hexane), tributyltin chloride and multi-wall carbon nanotubes (O.D. × L 6–9 nm × 5 μm, >95% carbon) were purchased from Sigma-Aldrich. Hydrobromic acid was purchased from Acros. Tetrahydrofuran was purchased from Fisher and purified over benzophenone and sodium. Alcoholic beverages were of commercial types.

2.2 Apparatus

Electrochemical measurements were performed with a Ivium CompactStat (The Netherlands) potentiostat in a cell equipped with three electrodes. Electropolymerization was performed with a Voltalab 50 potentiostat in a three-electrode cell consisting of graphite electrode (RingsdorffWerke GmbH, Bonn, Germany, type RW001, 3.05 mm diameter and 13% porosity) as the working electrode. A platinum wire as the counter electrode, and a Ag wire as the pseudo-reference electrode were employed. In order to perform the spectroelectrochemical studies of polymer films a Varian Cary 5000 UV-Vis spectrophotometer was used. For surface analysis of the ethanol electrode, scanning electron microscopy (SEM) (JEOL JSM-6400 model) and X-ray photoelectron spectroscopy (XPS) (PHI 5000 Versa Probe (F ULVACPHI, Inc., Japan/USA)) with monochromatized Al Kα radiation (1486.6 eV) 10 as an X-ray anode at 24.9 W were used. 1H NMR and 13C NMR spectra were recorded in DMSO-d6 on a Bruker Spectrospin Avance DPX-400 spectrometer and the chemical shifts were expressed in ppm relative to DMSO-d6 and $CDCl_3$ as the internal standard. Infrared (IR) spectra were recorded on a Varian 1000 FT-IR spectrophotometer in KBr pellets. A Waters Synapt MS System HRMS (High Resolution Mass Spectrometer) was used to confirm the synthesized materials.

2.3 Synthesis of 4,7-dibromo-2(4-nitrophenyl)-1*H*-benzo[*d*]-imidazole (4)

To synthesize the corresponding acceptor group, firstly, benzothiadiazole (1) was brominated and further reduction of this unit was carried out in the presence of $NaBH_4$ as reported in the literature.[16,17] 3,6-Dibromobenzene-1,2-diamine (3) (1.0 g, 3.7 mmol) was dissolved in 7.0 mL acetonitrile (ACN). Subsequently, hydrogen peroxide (H_2O_2) (2.0 mL, 20 mmol) was added into the mixture. After dropwise addition of 4-nitrobenzaldehyde (0.36 mL, 3.7 mmol) and ammonium cerium(IV) nitrate (0.2 g, 0.4 mmol) to the mixture, the resulting solution was stirred overnight at room temperature. Afterwards, the reaction mixture was poured into the ice/water mixture and the solid was filtered. The residue was washed with acetonitrile and the target product was yielded as a pale beige solid (4) (0.5 g, 1.26 mmol, 36%) (Scheme 3).

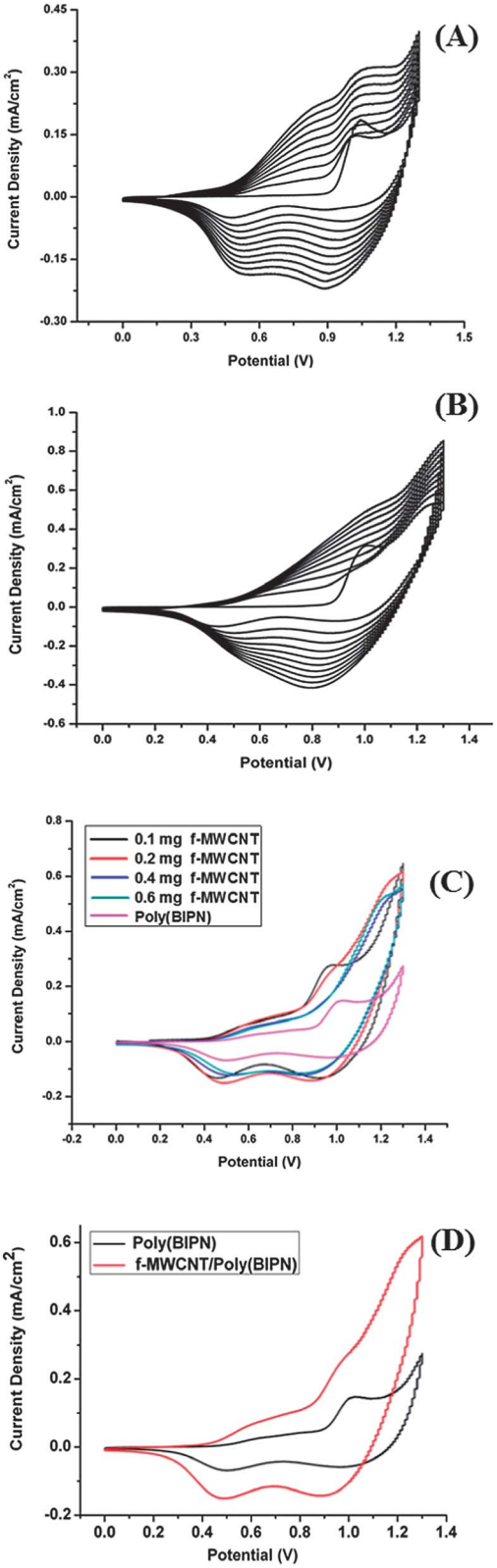

Fig. 1 Repeated potential scan polymerization of (A) poly(BIPN) and (B) f-MWCNT/poly(BIPN) in 0.1 M $LiClO_4/NaClO_4$, DCM–ACN (5 : 95, V/V) solution at 100 mV s^{-1}. (C) Cyclic voltammograms of poly(BIPN) and f-MWCNT/poly(BIPN) at different f-MWCNT concentrations. (D) Cyclic voltammograms of poly(BIPN) and optimum f-MWCNT/poly-(BIPN) electrode in 0.1 M $LiClO_4/NaClO_4$, DCM–ACN (5 : 95, V/V) solution at 100 mV s^{-1}.

1H NMR (400 MHz, d-DMSO): δ 13.67 (s, 1H), 8.59 (d, 2H, J = 8.91 Hz), 8.42 (d, 2H, J = 8.92 Hz), 7.45 (s, 2H). 13C NMR (d-DMSO): 159.2, 149.3, 146.9, 133.5, 127.1, 122.6, 121.9, 108.0.

2.4 Synthesis of 2-(4-nitrophenyl)-4,7-di(thiophen-2-yl)1*H*-benzo[*d*]imidazole (BIPN)

4,7-Dibromo-2(4-nitrophenyl)-1*H*-benzo[*d*]imidazole (0.5 g, 1.3 mmol) and tributyl(thiophen-2-yl)stannane (2.4 g, 6.5 mmol) were synthesized according to a previously described method.[18] After the mixture was heated under argon atmosphere, bis-(triphenylphosphine)palladium(II) dichloride was added as the catalyst.[19] The reaction proceeded under reflux in argon atmosphere for 16 hours and ended with TLC monitoring after 16 hours. The solvent was evaporated and the product was purified by column chromatography and obtained as an orange solid (eluent: DCM–hexane, 3 : 1) (0.12 g, 0.3 mmol, 20%) (Scheme 3).

1H NMR (400 MHz, d-DMSO): δ 13.02 (s, 1H), 8.66 (d, 2H, J = 7.97 Hz), 8.45 (d, 2H, J = 8.94 Hz), 8.25 (s, 1H), 7.71–7.66 (m, 4H), 7.41 (d, 1H, J = 6.76 Hz), 7.32–7.25 (m, 2H). 13C NMR ($CDCl_3$): δ 147.1, 146.9, 143.7, 143.5, 138.3, 133.6, 126.5, 125.6, 124.3, 124.2, 124.1, 122.7. HRMS: calculated $[M]^+$ = 404.0527, measured $[M]^+$ = 404.0522.

2.5 MWCNT functionalization

Pristine MWCNT (0.3 g) was dispersed in concentrated nitric acid (HNO_3, 70 mL, 65%) and refluxed for 48 hours. Afterwards, the reaction mixture was cooled to room temperature and filtered under vacuum. The residue was washed with distilled water until the pH of the solution became neutral. Then, the thin film of f-MWCNTs was dried at 80 °C overnight and a black powder was obtained.[20]

2.6 Biosensor preparation

For the construction of the bioactive layer on the graphite electrode, graphite rods were polished on emery paper and washed completely with distilled water. f-MWCNT modified poly(BIPN) based electrodes were prepared as follows: the functionalized MWCNT (0.2 mg) was mixed in 0.001 M BIPN monomer solution in 0.1 M $NaClO_4/LiClO_4$/DCM : ACN (5 : 95) by ultrasonication for 4 h. The f-MWCNT comprising a conducting polymer layer was obtained through electropolymerization by cycling the potential between 0 and 1.3 V at a scan rate of 0.1 V s^{-1} on the graphite electrode. The electrode was washed with distilled water to remove the organic impurities. After successful deposition of f-MWCNT/poly(BIPN) by cyclic voltammetry, 10 μL of AOx solution (50 mM pH 7.0 sodium phosphate buffer solution containing 3 U AOx, 0.4 M *N*-(3-dimethylaminopropyl)-*N*-ethylcarbodiimide hydrochloride (EDC) and 0.1 M *N*-hydroxysuccinimide (NHS)) was spread over the modified graphite electrode and left to dry for 3 h at room temperature. The enzyme electrode was stored at 4 °C overnight. Finally, to get more uniform films, it was rinsed with distilled water. Hence, we obtained adherent, robust and higher response signals *via* an efficient combination of enzyme molecules with modified electrode containing f-MWCNT/poly(BIPN)/AOx successfully.

2.7 Amperometric biosensor measurements

Amperometric studies were achieved in a reaction cell containing 10 mL phosphate buffer solution (50 mM, pH 7.0) under continuous stirring. After each measurement, working buffer solution was refreshed and electrodes were washed with distilled water and kept in phosphate buffer solution (50 mM, pH 7.0). A decrease in oxygen level as a result of enzymatic reaction was monitored at −0.7 V *vs.* Ag in phosphate buffer. After background current reached a steady state, freshly prepared ethanol solution was injected into the medium and the current change was recorded. All the experiments were carried out at ambient conditions. Measurements of amperometric analyses were calculated as the average of three measurements and standard deviations were given as ±SD.

3. Results and discussion

3.1 Electrochemical polymerization of f-MWCNT/BIPN

The purified f-MWCNT (0.2 mg) was mixed with 0.001 M BIPN monomer solution in the 0.1 M $NaClO_4$/$LiClO_4$/DCM : ACN (5 : 95) electrolyte/solvent system by ultrasonication for 4 h at room temperature. After this treatment a black suspension was obtained as depicted in Scheme 2. During this step, functional groups of BIPN were adsorbed on the f-MWCNT surface with the help of π–π conjugation of BIPN. The polymer film of f-MWCNT/poly(BIPN) was potentiodynamically coated on the graphite electrode with 10 scans between 0 V and 1.30 V *versus* Ag wire pseudo-reference electrode *via* cyclic voltammetry with a scan rate of 100 mV s^{-1} (Fig. 1(B)).

Charges involved in the film formation were calculated as 0.32 mC (thickness, 7.0 nm) for pristine poly(BIPN) and 0.50 mC (thickness, 11.0 nm) for f-MWCNT/poly(BIPN). This difference can be related to the presence of f-MWCNTs on the electrode surface. Moreover oxidation potentials for monomer, polymer and f-MWCNTs incorporating the polymer can be calculated from cyclic voltammograms. From Fig. 1(A) and (B), E_{ox}^{mon} were calculated using the first cycle of repeated potential scan polymerizations as 1.05 V and 0.99 V, respectively. Insertion of functionalized MWCNTs into poly(BIPN) has a significant effect on both electroactivity (current, charge) and oxidation potentials. After inserting f-MWCNTs, ΔE_{ox} was calculated as 60 mV from the cyclic voltammetry results. A tremendous increase in the current density of f-MWCNTs compared to the pristine one also proves the previously discussed argument (Fig. 1(A) and (B)). Therefore, it can be concluded that insertion of f-MWCNTs into the corresponding polymer solution increases the electroactivity.[5,25]

CPs can be used as immobilization matrices due to their good electrochemical and physical properties. Moreover, thanks to their easy decoration with functional groups during their synthesis, more powerful and robust polymeric films can be achieved for desirable enzyme immobilization. On the other hand, CNTs have received considerable attention as an electrode material due to their good electrocatalytic properties. As seen in Fig. 1(D), addition of an optimum amount of modified CNTs (0.2 mg) improved biosensor performance. In Fig. 1(D), the second cycles for the polymerizations of BIPN and f-MWCNT/poly(BIPN) were seen. The amounts and conditions in electropolymerization were kept constant whereas electropolymerization shown with a black line depicts only the polymerization of the monomer.

CNTs have high specific surface area making them promising candidates for the construction of a highly porous skeleton.[26] Especially, carboxylic acid group functionalized CNTs have advantages in the immobilization of biomolecules through covalent bond formation and hence, highly specific biomolecule detection can be achieved. This combination offers a useful platform for immobilizing biomolecules to enhance sensor performances. It also provides a good interaction between the active site of the enzyme and CNTs inside the polymer layer. These results were evidenced by cyclic voltammetry where higher amperometric responses and charge involved in the film formation were obtained compared to the matrix without CNTs (Fig. 1(C)). The formation of f-MWCNT/poly(BIPN) has been explored for a possible improvement in the electrical properties

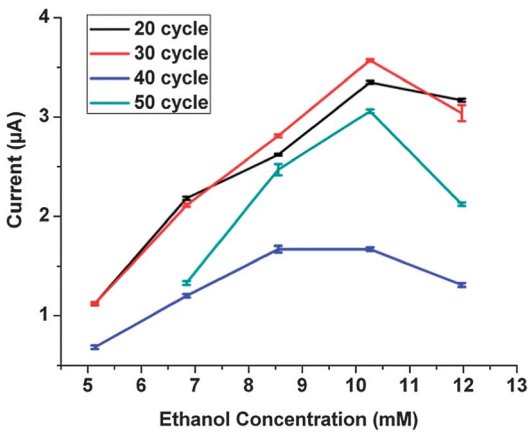

Fig. 2 Effect of cycle number (in phosphate buffer, 50 mM, pH 7.0, 25 °C, −0.7 V). Error bars show the standard deviation (SD) of three measurements.

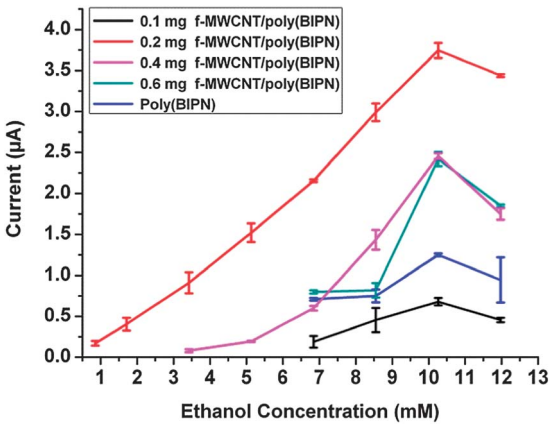

Fig. 3 Effect of f-MWCNT amount on the biosensor response (in 50 mM phosphate buffer, pH 7.0, 25 °C, −0.7 V). Error bars show the standard deviation (SD) of three measurements.

of polymers. Polymerization changes with the introduction of f-MWCNTs into the monomer solution as seen in the second cycles of each electropolymerization (Fig. 1(C)). The effect of carbon nanotube addition can be clearly seen and is discussed above. However, when the amount of f-MWCNTs increases in the monomer solution (0.4 and 0.6 mg), the charge deposition of the films decreases. This may be associated with the defect formation in the polymer film due to the excess presence of CNTs on the electrode surface. The polymer chains may form shorter or the stacking of the chains may be destroyed; hence, the ordered structure of the polymeric film may be affected after a certain amount of f-MWCNTs during polymerization.

3.2 Optimization studies

The thickness of the polymer/f-MWCNT layer can be adjusted with the scan number during electropolymerization. To investigate the effect of the film thickness on a biosensor performance, electrodes were prepared with different scans and biosensor responses were determined (Fig. 2). Since the released electrons during the enzymatic reactions should be properly transferred to the transducer, the thickness of the film is very important. To keep the enzymatic layer stabilized on the electrode surface, a proper thickness is desired. On the other hand, enzyme molecules together with the modified layer due to the covalent and physical binding may leach from the surface. In a small thickness huge protein molecules could not be stabilized on the electrode surface. In order to investigate the effect of conducting polymer and functionalized carbon nanotube layer thickness, an optimum concentration (0.2 mg carbon nanotube in 2 mL monomer solution) was used in polymerization on the graphite electrode *via* using different scan numbers (20, 30, 40 and 50 scans). During these experiments, other than polymeric layer thickness, all other parameters were kept constant. The optimum value was found with 30 scan electropolymerization.

For the investigation of sensor coating composition, different compositions of f-MWCNT/poly(BIPN) suspension were tested. In these experiments, other than CNT amount, all other parameters were kept constant. For this reason, five different biosensors were prepared on the graphite electrode in the 0.1 M $NaClO_4$/$LiClO_4$/DCM : ACN (5 : 95) electrolyte/solvent system at room temperature *via* scanning the potential between 0 V and 1.3 V (*vs.* Ag reference electrode) with a scan rate of 100 mV s^{-1} for 30 cycles. Fig. 3 shows that the response to ethanol does not continually increase or decrease with the amount of nanotubes incorporated. Higher carbon nanotube amounts caused decrease in the responses and this might be due to the diffusion problem for the substrate as well as limited orientation for the enzyme molecules. High amounts of CNTs in the films allow electrical communication but at some point, the response is limited by the electron transfer from the enzyme to the polymer's redox center. Moreover, in such excess amounts, the polymer coating on the electrode surface loses its quality due to the defects in the polymer chains in the presence of CNTs. This result is in accordance with previous studies.[27] The large surface area due to the presence of CNTs on the transducer surface may cause an increase in the background current. In similar works,[27,28] after some point, the introduction of CNTs into the surface affects signal in an unfavorable manner resulting in a decrease in biosensor responses.

On the other hand, with low amounts of CNTs, enzyme molecules could not be fixed properly onto the poly(BIPN) coated electrode which resulted in lower responses and leaching of enzyme from the electrode surface. Fig. 3 shows that the optimum f-MWCNT amount was found to be 0.2 mg in 0.001 M monomer solution. Maximum interaction and satisfactory immobilization of the enzyme molecules were achieved with this amount. The effect of f-MWCNT amount is also in accordance with the results in cyclic voltammograms taken in different amounts of f-MWCNT. The most electroactive coating also gives the best results in amperometric studies. This shows the reliability and effectiveness of the prepared matrix.

The surface area of the modified electrode plays an important role in the construction of biosensors. So, for the determination of the effective surface area, experiments were done and estimated using the Randles–Sevcik equation. Using the

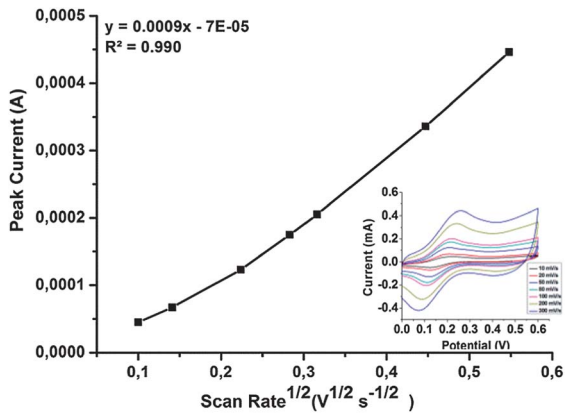

Fig. 4 The effect of peak currents for the determination of the working surface area. Inset: Cyclic voltammograms of working electrode in 5.0 mM $Fe_3(CN)_6^{3-}$ solution in 0.1 M KCl and 50 mM pH 7.0 phosphate buffer at scan rates 10–300 mV s^{-1}.

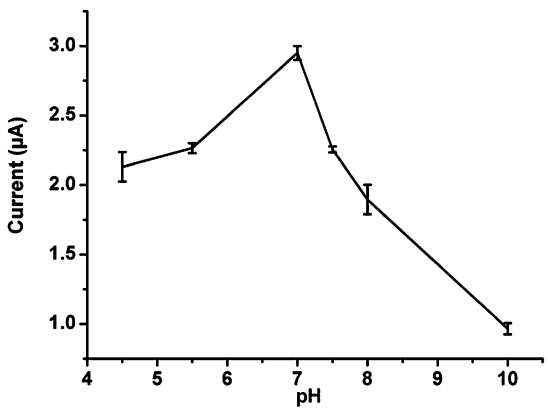

Fig. 5 Effect of pH (50 mM sodium phosphate buffer at pH 4.5, 5.5, 7.0, 7.5 and 50 mM sodium bicarbonate buffer at pH 8.0 and 10.0, 8.55 mM ethanol, 25 °C, −0.7 V). Error bars show the standard deviation (SD) of three measurements.

equation, the surface area is proportional to $I_p/v^{1/2}$. To calculate this proportion, cyclic voltammograms of the bare and also modified electrode were measured in a mixture solution of 0.1 M KCl and 5 mM $K_3Fe(CN)_6$ under various scan rates such as 10, 20, 50, 80, 100, 200 and 300 mV s^{-1}. The applied potentials are between 0 and 0.6 V. As shown in Fig. 4 the linearity for the modified electrode is very good. Using the slope, the modified electrode surface area was found to be 1.078×10^{-1} cm^2 which is higher than the bare electrode surface area. This result clearly shows that the modified electrode surface was used for the efficient immobilization matrix.

The effect of different amounts of AOx on the amperometric response was also investigated in the presence of 8.55 mM ethanol. Different amounts of the enzyme (2 U, 3 U, 4 U and 5.2 U) were immobilized on the modified electrode surface and the highest signals were recorded by the biosensor with 3 U AOx in the bioactive matrix. Higher enzyme amounts caused leaching from the surface. Hence, for the further experimental steps a biocomposite matrix with an optimum amount of AOx was used.

Since enzyme stability is highly affected by certain environmental conditions, pH is the one of the main factors for biosensors. The effect of pH on the amperometric biosensor response was examined using 50 mM phosphate buffer solution in a range of pH 4.5–10 in the presence of ethanol as the substrate (8.55 mM). Maximum current responses were found at pH 7 (Fig. 5). If the pH of the environment is extremely out of range, protein can be denatured.[29]

3.3 Characterization

3.3.1 Scanning Electron Microscopy (SEM) studies. Scanning electron microscopy (SEM) was used to characterize the surface morphologies of modified electrodes. Fig. 6 shows SEM

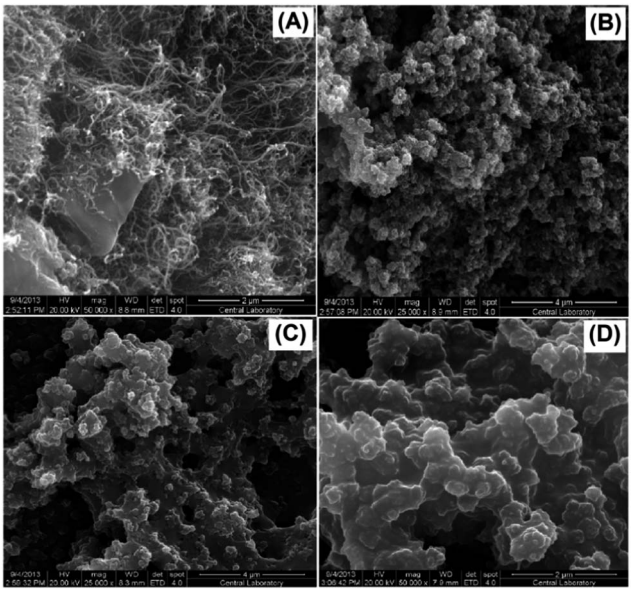

Fig. 6 Surface characteristics of (A) only f-MWCNT, (B) only poly-(BIPN), (C) f-MWCNT/poly(BIPN) and (D) f-MWCNT/poly(BIPN)/AOx *via* SEM images.

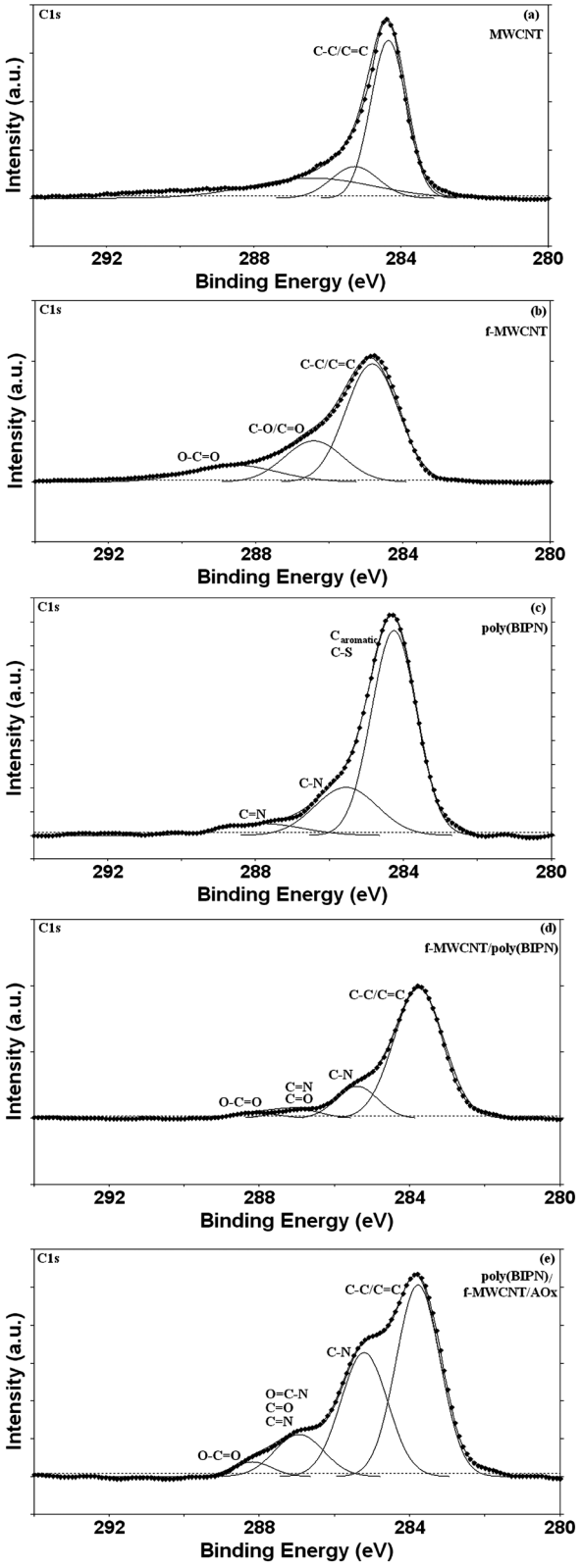

Fig. 7 XPS C1s spectra of (a) pristine MWCNT, (b) f-MWCNT, (c) poly-(BIPN), (d) f-MWCNT/poly(BIPN) and (e) AOx immobilized f-MWCNT/poly(BIPN).

images of the conducting polymer coated graphite electrode poly(BIPN), f-MWCNT, poly(BIPN)/f-MWCNT and poly(BIPN)/f-MWCNT/AOx modified electrode surfaces, respectively. The surface morphology of the only f-MWCNT film (Fig. 6(A)) shows typical fibrous shape. For the pure polymer, Fig. 6(B) depicts the porous and cauliflower structure of a typical conducting polymer. In Fig. 6(A–C), it can be observed that the poly(BIPN) and f-MWCNT films reveal a morphology composed of uniform surface due to the good interaction between nanotubes and polymer's functional groups. This structural difference may explain different electrochemical behaviors of poly(BIPN) and f-MWCNT/poly(BIPN). As shown in Fig. 6(C) the deposited poly(BIPN) is mostly wrapped around the f-MWCNTs. This fact leads to a higher conductivity and improved electrochemical properties for the films. The polymer and carbon nanotubes uniformly cover the electrode surface and provide porosity and a network. Such a surface design acts as a perfect layer for enzyme immobilization which is also supported by the amperometric results. Enzyme molecules are well-adhered on the coated electrode surface with the help of covalent binding due to the functional groups. In Fig. 6(D), after immobilization of AOx onto the modified electrode, the morphology of the surface changed drastically. This change can be related to the interaction between the functional groups of conducting polymer/nanotubes and protein molecules. In addition to this, comprehension of enzyme molecules through the structure of nanotubes may form electrostatic interactions between the enzyme and poly(BIPN). This clearly shows that the enzyme was well-organized onto the modified surface.

3.3.2 X-ray photoelectron spectroscopy (XPS) studies. Using X-ray photoelectron spectroscopy, carboxylic acid functionalization of MWCNTs and preparation of biolayer on the electrode surface were monitored (Fig. 7(a–f)). All samples were degassed before each analysis. XPS data recorded for each sample were used to determine the specific binding energies *via* a fitting program. Fig. 7(a) and (b) depict the C1s spectra of MWCNT and f-MWCNT which could be resolved into several characteristic peaks. In addition to the peak at 284.8 eV representing unmodified carbon (C–C/C=C), the peaks at 286.4 and 288.7 eV are attributed to C–O/C=O and O=C–OH confirming the functionalization and introduction of the COOH substituent.[30] The peaks at 285.3 and 286.4 eV for unmodified MWCNT (which was used as-received in XPS studies) can be related to sp^3-hybridized carbon atoms and structural defects on the nanotube structure[31] and atmospheric oxidation or remaining oxides arising from the purification process of MWCNTs. These results are also coherent with the FTIR results.[30] Moreover, the polymerization and immobilization were also confirmed *via* XPS studies using the C1s spectrum (Fig. 7(c)). In the C1s spectrum of conducting polymer, the peak at 284.3 eV can be attributed to aromatic carbons in the structure of polymer backbone and benzene unit and C–S in thiophene units.[32] The peaks at 285.6 and 287.8 eV belong to C–N in benzimidazole and C–N bond of nitrobenzene group, and C=N in benzimidazole ring, respectively.[33,34] XPS of the f-MWCNT containing conducting polymer coated surface was also performed. Due to the presence of f-MWCNT aromatic units in the polymer, the peak at 284.0 eV is attributed to C–C/C=C. 285.4 eV shows the C–N bond. 287.0 eV indicates the benzimidazole unit and nitrobenzene presence as well as C=O bond in the f-MWCNT structure. In addition, a peak at 288.1 eV belongs to the O=C–OH substituent which confirms the presence of f-MWCNTs within the polymeric structure (Fig. 7(d)).

Successful immobilization of alcohol oxidase and covalent binding were confirmed *via* XPS results. In the C1s spectrum of the enzyme immobilized f-MWCNT/conducting polymer coated electrode surface, the increase in intensity of the peak at 285.2 eV shows the presence of C–N bond, imidazole, nitrobenzene and MWCNT.[30,35] The peak at 287.1 eV is attributed to the O=C–N bond which confirms the covalent immobilization *via* amide bond formation between carboxylic acid groups of the f-MWCNT and amino groups of the enzyme molecules.[30] Besides, the increase in the signal at 288.2 eV confirms the presence of carboxylic acids due to f-MWCNT and protein molecules.

3.3.3 Fourier transform infrared (FTIR) studies. FTIR spectra of pristine MWCNT, functionalized MWCNT, poly(BIPN) and poly(BIPN) with f-MWCNT are represented in Fig. 8. In pristine MWCNTs, the characteristic peak of C=C vibration was observed at 1560 cm^{-1} (Fig. 8(a)).[21] After functionalization of MWCNTs, three new peaks appeared at 3440 cm^{-1}, 1730 cm^{-1} and 1400 cm^{-1} referring to O–H stretching, C=O stretching and O–H bending vibrations, respectively (Fig. 8(b)).[22] This result clearly shows that the –COOH group was successfully obtained on the surface of MWCNTs. Fig. 8(c) shows the spectrum of electropolymerized poly(BIPN). The peak at 3392 cm^{-1} indicates the characteristic N–H stretching of imidazole moiety. Another observation related to the aromatic imidazole ring is the C–N stretching peak at 1402 cm^{-1}.[23] The

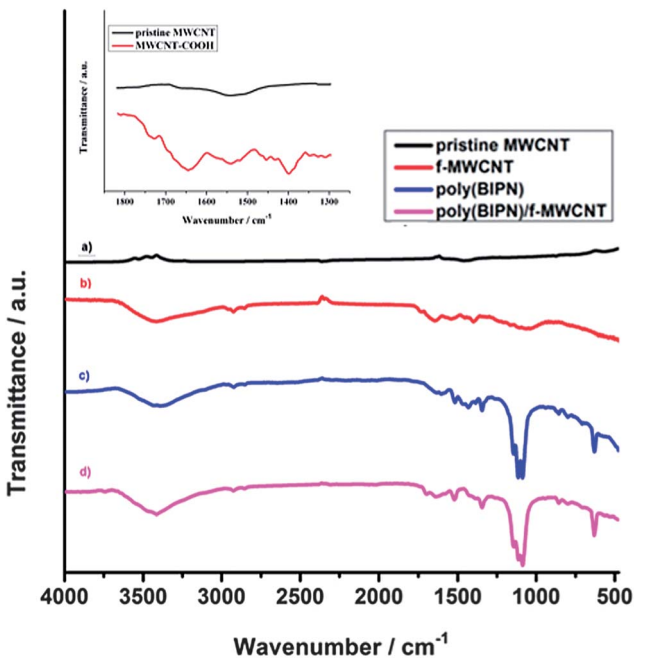

Fig. 8 FTIR spectra of (a) pristine MWCNT, (b) f-MWCNT, (c) poly(BIPN) and (d) poly(BIPN)/f-MWCNT (1300–1800 cm^{-1} interval for pristine MWCNT and f-MWCNT given as the inset).

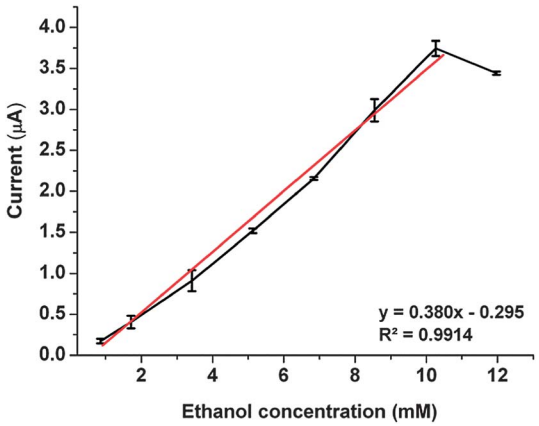

Fig. 9 Calibration curve for ethanol (in 50 mM phosphate buffer, pH 7.0, 25 °C, −0.7 V). Error bars show the standard deviation (SD) of three measurements.

symmetrical stretching vibrations of nitro group are assigned to the peaks at 1379 cm^{-1} and 1344 cm^{-1}.[24] The C–H bending vibrations are summarized as 1143 cm^{-1}, 1111 cm^{-1} and 1086 cm^{-1} in-plane, 856 cm^{-1} and 798 cm^{-1} out of plane (Fig. 8(c)).[24] The structure of BIPN was also characterized by 1H NMR spectroscopy. In Fig. 8(d) O–H and N–H bending for f-MWCNTs and poly(BIPN) overlapped and represented as a broad peak at 3414 cm^{-1}. The C═O stretching peak was shifted from 1730 cm^{-1} to 1697 cm^{-1} as a result of the hydrogen bonding formation between –COOH and $-NO_2$ groups due to the presence of poly(BIPN) (Fig. 8(d)).[22]

3.4 Analytical properties, repeatability and storage stabilities of the ethanol biosensor

After all optimizations, biosensor responses for different amounts of ethanol were recorded to construct a calibration curve (Fig. 9). The limit of detection (LOD) was calculated as 0.17 μM based on $S/N = 3$. Some characteristic parameters including kinetic parameters (K_M^{app}, I_{max}) and sensitivity were calculated as 16.949 mM, 3.31 μA and 476 μA mM^{-1} cm^{-2} respectively. A perfect linearity was obtained between 0.855 mM and 11.97 mM ethanol in 50 mM sodium phosphate pH 7.0 buffer as given in Fig. 9. SD and the RSD were calculated as 0.067 and 2.38%, respectively. K_M^{app} and I_{max} values were calculated from the Lineweaver–Burk plot. A low K_M^{app} value is an indication of higher substrate affinity. Hence, with the help of the modified layer, immobilized enzyme molecules exhibit higher affinity toward ethanol. Moreover, the K_M^{app} value for the poly(BIPN)/f-MWCNT/AOx biosensor is extremely smaller than the ones reported in earlier studies (Table 1). This shows the effectiveness and success of the immobilization matrix, sensitivity of the biosensor and applicability in other operations. In recent years, several studies related to conducting polymer and carbon nanotube based ethanol biosensors were investigated in the literature and are summarized in Table 1.

Over the past few years, various approaches on carbon nanotubes, especially the functionalized ones, have been developed in order to improve the communication between the active site and electrode. Moreover, carbon nanotube based biosensors exhibit higher sensitivity, better stability and especially a broad linear response range. For example, a polyaniline/carboxy functionalized MWCNT nanocomposite was developed as an interesting biosensor.[7] Functionalized carbon nanotubes were mixed with chemically polymerized polyaniline, stirred and filtered to get the composition. Then the composition was mixed with the HRP enzyme and transferred to the Au electrode surface. It was proved that the linear range was expanded from 26–8000 μM to 886 μM to 10 mM with the help of both carbon nanotubes and conducting polymer.[7] Liu *et al.* demonstrated that the bio-composite film constructed *via* the layer by layer technique containing MWCNT, chitosan and PAMAM nanocomposite could be used as dopamine and uric acid sensor with improved sensitivity and very extensive linear range.[41] An amperometric lactate biosensor based on conducting polymer and MWCNT composite on a gold electrode was reported by Rahman *et al.*[42] Results of this biosensor proved that sensitivity, stability as well as reproducibility had been improved significantly *via* using MWCNTs. With this information, the use of nanotubes for the construction of biosensors has been very promising to obtain fast response and an efficient biosensor. Also in our case the use of f-MWCNTs improved the performance of biosensors as well as lowered the detection limit compared to the pristine poly(BIPN) biosensor.

There are multistep applications of similar methods for the preparation of CNT containing surfaces in the literature.[43,44] To the best of our knowledge, one step preparation of MWCNTs and conducting polymer composite biolayer is rare in the literature.[45–48] Hereby, a novel monomer for conducting polymer was synthesized and applied for the formation of a composite layer with MWCNT. The combination of a novel conducting polymer of BIPN with functionalized MWCNTs is not explored for the detection of ethanol. The novel monomer is dissolved in organic solvents; nevertheless, the system works well. The one step procedure is easy to apply, simple, effective and homogeneous. Moreover, the preparation of alcohol biosensors with

Table 1 Comparison of biosensors, using the same technique, examples from the literature involving ethanol biosensors. (NR: not reported.)

Immobilization matrix	Linear range	Sensitivity	Ref.
Carbon paste matrix/AOx-HRP-osmium	250–2000 μM	NR	36
MWCNT-Nafion/Aox/Au electrode	8.0–42 μM	3.0 μA mM^{-1}	37
Hydrogel/AOx/platinum electrode	0.02–3.75 mM	10.6 nA mM^{-1}	38
Chitosan/AOx-eggshell membrane	60–800 μM	NR	39
Poly(neutral red) (PNR)/carbon film electrode	0–1.0 mM	171.8 nA mM^{-1}	40
f-MWCNT/poly(BIPN)/AOx	0.855 mM/11.97 mM	476 μA mM^{-1} cm^{-2}	This work

Table 2 Substrate selectivity of the biosensor (amperometric response of methanol accepted as 100%)

Substrate	Activity (%)
Ethanol	97
Methanol	100
2-Propanol	32
tert-Butanol	2

this method brings novelty and improved results with the help of effective surface design and modification.

To determine substrate selectivity of the biosensor, 8.56 mM of various substrates such as ethanol, methanol, 2-propanol and *tert*-butanol were tested. The results indicated that the biosensor responded to primary aliphatic alcohols, and the maximum responses were obtained for ethanol (Table 2). Compared with the primary aliphatic alcohols, the biosensor response decreased with an increasing chain length. The decrease can be attributed to steric effects of branched alcohols which make it hard to reach the biosensor surface. Hence, the proposed biosensor was very suitable for ethanol determination.[49]

The lifetime of the modified electrode was determined by measuring the amperometric response for 30 days. During the experiments, an activity loss of 2% was observed on the 30th day. This result is the superior for the construction of a long-life biosensor. The biosensor was kept at +4 °C when not in use.

In addition, investigation of the effects of various materials as interferents was carried out with the proposed biosensor. Possible interferents like ascorbic acid, cholesterol, glucose and urea (between 1 mM and 10 mM) were studied as the substrate in a reaction cell containing 50 mM, pH 7.0 phosphate buffer solution. Amperometric measurements were done under optimized working conditions by applying −0.7 V where no interference effect was detected.

During the enzymatic reactions, oxygen consumption can be determined at −0.7 V. When a potential of −0.7 V is applied to the cathode, a current proportional to the oxygen content is generated. During the catalytic reactions of oxidase enzymes, oxygen is consumed. Hence this proposed biosensor can be used in various applications even in the presence of such interferents in the analyte.

3.5 Sample application

To investigate the performance and reliability of the constructed biosensor, it was tested for various beverages. Real samples with no dilution were analyzed with f-MWCNT/poly-(BIPN)/AOx biosensor (Table 3). The experiments were carried out at optimum conditions. Traditional conventional methods are often slower and with high cost which utilize undesirable routine analysis whereas this proposed biosensor has the advantages such as simple measurement procedure, easy fabrication and efficient sensitivity and selectivity. Thus, construction of this enzyme based amperometric biosensor has an importance for the detection of ethanol samples. Results prove that there exists no significant difference between the two methods showing the reliability and accuracy of the biosensor. Hence, our system enables us to determine ethanol with an acceptable accuracy and rapid analysis.

Table 3 Ethanol detection in various samples

Sample	Label value (%)	Poly(BIPN)/f-MWCNT/AOx (%)	Relative error (%)
Y Brand Raki	40.0	39.9	0.25
J Brand Whiskey	40.0	43.0	7.50
B Brand Wine	21.0	21.3	1.43
S Brand Liquor	20.0	22.1	10.5

4. Conclusions

In this study, a novel conducting polymer was used for the construction of ethanol biosensors. The surface modifications of the proposed biosensor provide a perfect immobilization matrix for the alcohol oxidase enzyme. The fabricated biosensor exhibits excellent kinetic parameters such as K_M^{app}, I_{max}, low LOD and high stability. The combination of the CPs and nanotubes serves as a proper immobilizing platform for biomolecules and preserves enzyme activity for a long period. For the proper enzyme immobilization, it is known that the immobilization matrix has to preserve the stability and biological activities besides its orientation on the electrode surface. Moreover, it was successfully applied to the alcoholic samples with satisfactory results.

Notes and references

1 E. Sahin, P. Camurlu, L. Toppare, V. M. Mercore, I. Cianga and Y. Yagci, *J. Electroanal. Chem.*, 2005, **579**, 189.
2 Y. Xue, Z. Sheng, H. Zhao, Z. Wu, X. Li, Y. He and Z. Yuan, *Electrochim. Acta*, 2012, **59**, 256.
3 S. Tuncagil, S. Kıralp, S. Varis and L. Toppare, *React. Funct. Polym.*, 2008, **68**, 710.
4 S. Soylemez, F. E. Kanik, A. G. Nurioglu, H. Akpinar and L. Toppare, *Sens. Actuators, B*, 2013, **182**, 322.
5 K. E. Moore, B. S. Flavel, J. Yu, A. D. Abell and J. G. Shapter, *Electrochim. Acta*, 2013, **89**, 206.
6 (*a*) J. H. Huang, Y. J. Hong, Y. T. Chang, P. Chang and T. R. Yew, *J. Mater. Chem. B*, 2013, **1**, 5389; (*b*) Y. Liu, N. Lu, S. Poyraz, X. Wang, Y. Yu, J. Scott, J. Smith, M. J. Kim and X. Zhang, *Nanoscale*, 2013, **5**, 3872–3879.
7 M. Y. Hua, Y. C. Lin, R. Y. Tsai, H. C. Chen and Y. C. Liu, *Electrochim. Acta*, 2011, **56**, 9488.
8 B. F. Lu, G. Lingrong, J. M. Mohammed, W. Xin, G. L. Pengju, M. V. Lucia, C. Li and P. S. Ya, *J. Mater. Chem. B*, 2009, **21**, 139.
9 D. Carelli, D. Centonze, A. De Giglio, M. Quinto and P. G. Zambonin, *Anal. Chim. Acta*, 2006, **565**, 27.
10 (*a*) T. Malinauskas and A. Malinauskas, *Bull. Electrochem.*, 2005, **21**, 289; (*b*) A. M. Azevedo, D. M. F. Prazeres, J. M. S. Cabral and L. P. Fonseca, *Biosens. Bioelectron.*, 2005, **21**, 235–247.

11 H. B. Yildiz and L. Toppare, *Biosens. Bioelectron.*, 2006, **21**, 2306.
12 S. Cosnier and M. Holzinger, *Chem. Soc. Rev.*, 2011, **40**, 2146.
13 M. Tak, V. Gupta and M. Tomar, *J. Mater. Chem. B*, 2013, **1**, 6392.
14 L. Lili, F. Wei and P. Kehou, *Colloids Surf., B*, 2013, **102**, 124.
15 M. Situmorang, J. J. Gooding, D. B. Hibbert and D. Barnett, *Biosens. Bioelectron.*, 1998, **13**, 953.
16 B. A. Da SilveriaNeto, A. L. SantAna, G. Ebeling, S. R. Goncalves, E. V. U. Costa, H. F. Quina and J. Dupont, *Tetrahedron*, 2005, **61**, 10975.
17 Y. Tsubata, T. Suzuki, T. Miyashi and Y. Yamashita, *J. Org. Chem.*, 1992, **57**, 6749.
18 S. S. Zhu and T. M. Swager, *J. Am. Chem. Soc.*, 1997, **119**, 12568.
19 S. D. Uzun, N. A. Unlu, M. Sendur, F. E. Kanik, S. Timur and L. Toppare, *Colloids Surf., B*, 2013, **112**, 74.
20 V. Datsyuk, M. Kalyva, K. Papagelis, J. Parthenios, D. Tasis, A. Siokou, I. Kallitsis and C. Galiotis, *Carbon*, 2008, **46**, 833.
21 V. T. Le, C. L. Ngo, Q. T. Le, T. T. Ngo, D. N. Nguyen and M. T. Vu, *Adv. Nat. Sci.: Nanosci. Nanotechnol.*, 2013, **4**, 35017.
22 M.-Y. Hua, Y.-C. Lin, R.-Y. Tsai, H.-C. Chen and Y.-C. Liu, *Electrochim. Acta*, 2011, **56**, 9488.
23 Suryani, C.-M. Chang, Y.-L. Liu and Y. M. Lee, *J. Mater. Chem.*, 2011, **21**, 7480.
24 V. Arjunan, P. S. Balamourougane and S. S. Mohan, *Spectrochim. Acta, Part A*, 2009, **74**, 798.
25 K. E. Moore, B. S. Flavel, J. Yu, A. D. Abell and J. G. Shapper, *Electrochim. Acta*, 2013, **89**, 206.
26 F. Branzoi, V. Branzoi and A. Musina, *Prog. Org. Coat.*, 2013, **76**, 632.
27 S. Timur, U. Anik, D. Odaci and L. Gorton, *Electrochem. Commun.*, 2007, **9**, 1810.
28 J. Wang and M. Musameh, *Anal. Chim. Acta*, 2005, **539**, 209.
29 S. Suye, *Curr. Microbiol.*, 1997, **34**, 374.
30 T. Ramanathan, F. T. Fısher, R. S. Fisher, R. S. Ruoff and L. C. Brinson, *Chem. Mater.*, 2005, **17**, 1290.
31 W. H. Pana, S. J. Lue, C. M. Chang and Y. L. Liu, *J. Membr. Sci.*, 2011, **376**, 225.
32 F. E. Kanik, E. Rende, S. Timur and L. Toppare, *J. Mater. Chem.*, 2012, **22**, 22517.
33 W. Qingzhi, W. Yaping, H. Yufeng, G. Jianxin, C. Matthew, C. Shanshan, R. Yujie, J. Hengxing, L. Huifeng, W. D. Boukhvalov, D. P. Richard, W. B. Christopher and S. R. Rodney Ruoff, *Chem. Commun.*, 2013, **49**, 677.
34 S. A. Wohlgemuth, F. Vilela, M. M. Titirici and M. Antonietti, *Green Chem.*, 2012, **14**, 741.
35 M. Kesik, O. Kocer, F. E. Kanik, N. A. Unlu, E. Rende, E. A. Gurel, M. R. Rene, Y. A. Udum and L. Toppare, *Electroanalysis*, 2013, **25**, 1995.
36 A. R. Vijayakumar, E. Csöregi, A. Heller and L. Gorton, *Anal. Chim. Acta*, 1996, **327**, 223.
37 M. Das and P. Goswami, *Bioelectrochemistry*, 2013, **89**, 19.
38 N. G. Patel, S. Meier, K. Comman and G. C. Chemnitius, *Sens. Actuators, B*, 2001, **75**, 101.
39 G. Wen, Y. Zhang, S. Shuang, C. Dong and M. M. F. Choi, *Biosens. Bioelectron.*, 2007, **23**, 121.
40 M. M. Barsan and C. M. Brett, *Talanta*, 2008, **74**, 1505.
41 X. Liu, Y. Peng, X. Qu, S. Ai, R. Han and X. Zhu, *J. Electroanal. Chem.*, 2011, **654**, 72–78.
42 M. M. Rahman, J. A. S. Muhammad, M. A. Rahman and Y. B. Shim, *Anal. Biochem.*, 2009, **384**, 159–165.
43 L. Xiliang, J. K. Anthony, M. Aoife and R. S. Malcolm, *Anal. Chim. Acta*, 2006, **575**, 39.
44 S. Boncel, A. Zniszczoł, K. Szymańska, J. M. Białoń, A. Jarzębski and K. Z. Walczak, *Enzyme Microb. Technol.*, 2013, **53**, 263.
45 L. Ming, W. Yangping, L. Dong, Y. Ruirui, X. Jingkun and H. Haohua, *Sens. Actuators, B*, 2011, **159**, 277.
46 S. Yadav, R. Devi, S. Kumari, S. Yadav and C. S. Pundir, *J. Biotechnol.*, 2011, **151**, 212.
47 I. Cesarino, F. C. Moraes, R. V. Marcos, S. Lanza and A. S. Machado, *Food Chem.*, 2012, **135**, 873.
48 J. Wang and M. Musameh, *Anal. Chim. Acta*, 2005, **539**, 209.
49 A. R. Vijayakumar, E. Csöregi, A. Heller and L. Gorton, *Anal. Chim. Acta*, 1996, **327**, 223.